J Mater Sci: Mater Electron (2015) 26:2897–2904
DOI 10.1007/s10854-015-2775-z

Comparative investigations on dielectric, piezoelectric properties and humidity resistance of PZT–SKN and PZT–SNN ceramics

Fuli Zhu · Jinhao Qiu · Hongli Ji · Kongjun Zhu · Kai Wen

Received: 28 August 2014 / Accepted: 29 January 2015 / Published online: 27 February 2015
© Springer Science+Business Media New York 2015

Abstract Sodium was used to substituted for potassium in $Pb(Zr_{0.53},Ti_{0.47})O_3$–$Sr(K_{0.25},Nb_{0.75})O_3$ (PZT–SKN) based on the lead-free $(Na_{0.5}K_{0.5})NbO_3$ (KNN) piezoelectric ceramic and a new ceramic material $Pb(Zr_{0.53},Ti_{0.47})O_3$–$Sr(Na_{0.25},Nb_{0.75})O_3$ (PZT–SNN) was developed in order to improve the humidity resistance. PZT–SKN and PZT–SNN ceramics have been fabricated by the conventional solid-state reaction method at the sintering temperature of 1,150–1,225 °C for 2 h. The effects of SKN and SNN on the microstructure, piezoelectric properties and humidity resistance of the prepared ceramics have been systematically investigated and compared. The phase structures of the two ceramics are both tetragonal. With increasing of SKN/SNN, both the grain size and Curie temperature decrease. Among all compositions studied, the 0.99PZT–0.01SKN and 0.98PZT–0.02SNN sintered at 1,175 °C exhibited optimal comprehensive properties. Especially, the PZT–SNN has a higher humidity resistance than PZT–SKN. The optimal values of d_{33}, kp, ε_r and Tc for 0.98PZT–0.02SNN is 448pC/N, 0.63, 2,126.32 and 354 °C, respectively.

1 Introduction

Since the discovery of ferroelectric ceramics in the 1940s, lead-based perovskite-type solid solutions have attracted great interests due to their excellent dielectric,piezoelectric and electrostrictive properties [1]. As the predominant materials for piezoelectric applications,lead zirconate titanate (PZT) based ceramics are widely applied in multilayer ceramics capacitors (MLCC), ultrasonic motors, and especially, the multilayer piezoelectric actuators [2, 3]. For multilayer piezoelectric actuators, piezoelectric materials should possess a high field piezoelectric coefficient, d_{33}, of about 450pC/N with a Curie temperature above 300 °C so that the piezoelectric actuators could working in the room temperature or relative higher (about 150 °C) [4].

Nowadays, many investigations have been carried out to find candidate materials to fabricate multilayer piezoelectric devices. Some piezoelectric materials are added separately or together to the PZT system to form ternary or quaternary solid solutions, such as PZT–SKN [5], PZT–PMN [6], and PZT–PMN–PZN [7]. The $Pb(Zr_{0.53},Ti_{0.47})O_3$–$Sr(K_{0.25},Nb_{0.75})O_3$ (PZT–SKN) system were first reported by Helke et al. [8]. They prepared the PZT/SKN ceramics with the theoretical ionic complex $Sr(K_{0.25},Nb_{0.75})O_3$ using a conventional mixed oxide route and the maximum value of d_{33} ($\sim$445pC/N) was obtained with a Zr/Ti ratio of 52/48 sintered at 1,175 °C. Donnelly et al. [5] investigated the PZT ceramics with 0.02 SKN addition exhibit optimum piezoelectric properties for the $(1-x)$ PZT–xSKN system, which exhibits a high field d_{33} value of 750 pm/V and a high Curie temperature of 356 °C. Comparing other PZT-based materials, PZT–SKN has both large d_{33} values and high Cure temperature, becoming a promising material for multilayer piezoelectric actuator applications. However, the bulk is easy to show deliquescence once exposed to humidity due to the alkaline metal elements potassium. Potassium-contained compounds, such as potassium carbonate with high hygroscopicity, have been conventionally used as a desiccant in the chemical experiment. This feature limits the use of materials

F. Zhu · J. Qiu (✉) · H. Ji · K. Zhu · K. Wen
State Key Laboratory of Mechanics and Control of Mechanical Structures, Nanjing University of Aeronautics and Astronautics, Nanjing 210016, China
e-mail: qiu@nuaa.edu.cn

contain potassium. However, few researches on the humidity-resistance characteristic, which significantly affects their practical applications, have been carried out.

In this study, we substituted sodium for potassium in PZT–SKN based on the lead-free $(Na_{0.5}K_{0.5})NbO_3$ (KNN) piezoelectric ceramic and developed a new ceramic material: $Pb(Zr_{0.53},Ti_{0.47})O_3$–$Sr(Na_{0.25},Nb_{0.75})O_3$ (PZT–SNN). Comparable studies on the microstructures, dielectric, piezoelectric properties and specially humidity-resistance of these two materials have been investigated.

2 Experimental procedure

Ceramic compositions of $(1 - x)Pb(Zr_{0.53},Ti_{0.47})O_3$–$xSr(K_{0.25},Nb_{0.75})O_3$ and $(1 - y)Pb(Zr_{0.53},Ti_{0.47})O_3$–$ySr(Na_{0.25},Nb_{0.75})O_3$ (where $x = y$= 0.005, 0.01, 0.02, 0.03, 0.04 and 0.05) were prepared by conventional solid-state method used the powders of PbO, ZrO_2, TiO_2, $SrCO_3$, Nb_2O_5, K_2CO_3 and Na_2CO_3 (all with purity ≥99 %) as the raw materials. The powders were weighed according to the mole ratio and mixed in ethyl alcohol by ball-milling for 12 h with 1 % extra PbO added to compensate for PbO volatility. After drying, the PZT–SKN powders were calcined at 850 °C for 4 h and PZT–SNN calcined at 1,000 °C. Subsequently, the calcined powders were ball-milled again for 12 h and then a 5 wt% polybinyl alcohol (PVA) was added to the dried powders as a binder. After pressing into disks, the green pellets were heated at 650 °C to burnout the binder and then sintered at different temperatures (1,150, 1,175, 1,200 and 1,225 °C) for 2 h.

The bulk densities of the sintered ceramics were measured by the Archimedes method. Powder X-ray diffraction (XRD; D8 Advance) was used to identify the crystal structures and phases. The microstructure was observed using scanning electron microscopy (SEM, JSM-5610LV/Noran-Vantage). For measuring the piezoelectric and dielectric properties, the specimens were lapped into 0.8 mm thickness and then metallized with silver paste at 550 °C for 10 min. Subsequently, the ceramics were poled under a DC field of 3 kV/mm in silicon oil at 120 °C for 20 min. Properties were measured after the specimens were aged in air for 24 h. Piezoelectric constant (d_{33}) was measured using a static piezoelectric constant testing meter (Zj-3A, Institute of Acoustics, Chinese Academy of Science, Beijing, China), dielectric properties were measured using an impedance analyzer (HP4294A). The polarization–electric field (P–E) hysteresis loops were determined using a standard ferroelectric tester (TF analyzer 2000, aixACCT, Germany).

In order to determine the humidity-resistance characteristics of the ceramics, the samples were immerged into distilled water for different periods of time and we recorded the piezoelectric coefficient d_{33} (the samples used here are stored in a desiccator for 20 days after poling in order to minimize the aging effects).

3 Results and discussion

3.1 Microstructure analysis

The XRD patterns of the $(1 - x)$PZT–xSKN and $(1 - y)$PZT–ySNN sintered at 1,175 °C are shown in Fig. 1a. All compositions present the pure perovskite phase and both two ceramics are tetragonal phase structure. However, the combination of 2θ from 43° to 46° (Fig. 1b, c evidently show that when the potassium was substituted by sodium, the comparative intensity of the two splitting peaks of (002) and (200) around the 45° changed, that may because K^+ and Na^+ have different radius, when they occupy the A site, the lattice constant may vary by a small amount. Dewang et al. [9] investigated that by changing the amount of PZN and PNN, the comparative intensity of the two splitting peaks of (002) and (200) around the 45° have similar variation with us, which the author called typical tetragonal phase structure and untypical tetragonal phase structure.

Figure 2 depicts the fracture surface SEM micrographs and grain size of PZT–SKN/PZT–SNN with different SKN/SNN content sintered at 1,175 °C for 2 h, respectively. It indicates that all the ceramics show a good densification behavior. Meanwhile, the average grain size initially increases with increasing SKN/SNN content and then decrease. The maximum grain size is obtained at $x = 0.01/y = 0.01$. The declining trend from 0.01 to 0.05 matched perfectly with the one reported by Niall et al. [5]. Since there have been reported that grain growth is suppressed in PZT due to aliovalent substitutions such as La^{3+} (for Pb^{2+}) [10] or Nb^{5+} (for Zr^{4+}/Ti^{4+}) [11, 12], it is suggested this is a consequence of the "impurity drag" [10, 13] effect where dopant congregation near the grain boundary reduces its mobility leading to a reduction in the grain growth rate [5]. For SKN, considering the ionic radii of the constituent species, both the Sr and K occupy the A site in the perovskite lattice while only Nb occupies the B site. At the same time, because the charge compensation, one K^+ and Nb^{5+} can generate a half oxygen vacancy and a half lead vacancy, respectively. As a result, one SKN generate ¼ lead vacancy. This situation is the same to SNN. The vacancies as created by this doping are supposed to be bound to the impurity, so that they inhibit the mass transport and grain boundary mobility [14]. Considering the grain growth, the dopants keep the grain size small [1, 15, 16]. As a result, the grain size of $(1 - x)$PZT–xSKN/$(1 - y)$PZT–ySNN is decreased with increasing SKN/SNN content in the $x(y)$ range 0.01–0.05. However, the "solute

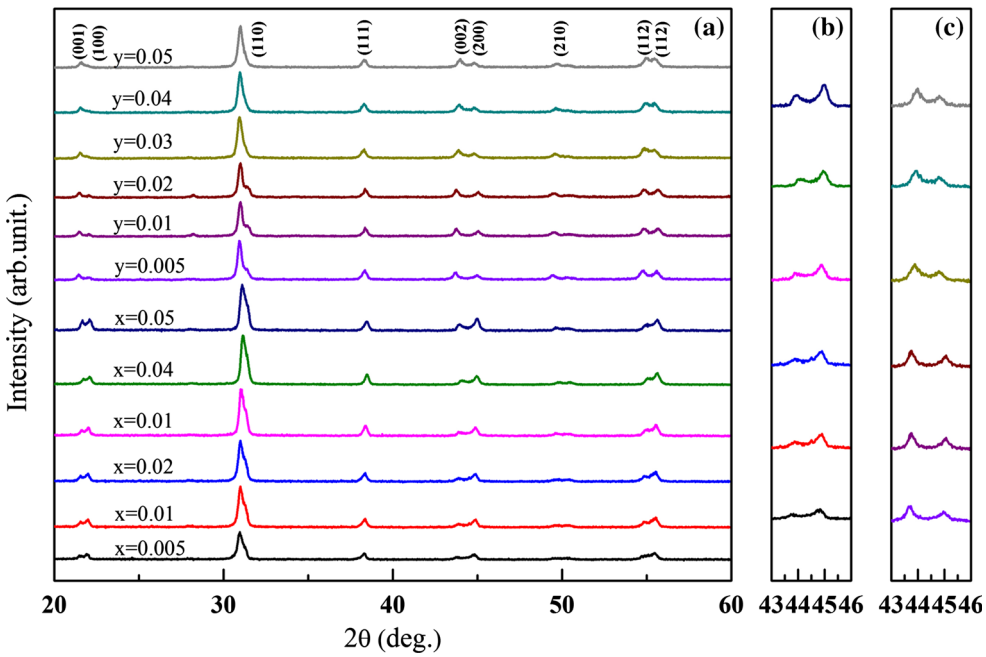

Fig. 1 **a** XRD patterns of $(1-x)Pb(Zr_{0.53},Ti_{0.47})O_3$–$xSr(K_{0.25},Nb_{0.75})O_3$ and $(1-y)Pb(Zr_{0.53},Ti_{0.47})O_3$–$ySr(Na_{0.25},Nb_{0.75})O_3$ in the 2θ range of 20°–60°,**b**, **c** enlarged (002) and (200) peaks within 43°–46° of PZT–SKN and PZT–SNN ceramics sintered at 1,175 °C

drag" effect [17] is puny when $x(y) = 0.005 - 0.01$ since the grain size increase and reach the maximum about 10 μm. In this study, we sintered four temperatures and find that the optimal performances are obtained at 1,175 °C, that means the SKN/SNN can lower the sintering temperature. When doping at low content (0.5 wt%), there exists little vacancy and the SKN/SNN's influence on sintering temperature plays a major role. If still sintered at original temperature, the relatively high temperature may promote grain grow and gain a larger grain size [18]. As the doping contents increasing, the "solute drag" effect becomes the predominant and the grain size diminishes gradually. Furthermore, we can see that grain size of PZT–SNN is larger than PZT–SKN, which means SNN has a greater effect than SKN in lowing the sintering temperature.

3.2 Ferroelectric, dielectric, and piezoelectric properties

The piezoelectric and dielectric properties of d_{33}, kp, and ε_r of $(1-x)$PZT–xSKN and $(1-y)$PZT–ySNN specimens as a function of the amount of SKN/SNN at various sintering temperatures for 2 h are shown in Fig. 3. Values of d_{33}, kp, and ε_r initially increase with SKN/SNN addition regardless of the sintering temperature, reaching a maximum values at both low level of doping content of 1 and 2 wt%, respectively, and then fall for higher concentrations. The improvement of the dielectric and piezoelectric properties of the ceramics is mainly due to the mechanisms of vacancy effect and grain boundary inhibition. During the poling process, the 90° domains gain further significance for virtually all 180° domains are oriented along the poling direction. When in low doping level, the vacancies caused by dopants facilitate the rotation of 90° domains and promote the motion of them, leading the enhancement of electromechanical properties [19]. Meanwhile, the vacancies lead to small distortion of the unit cell and increase the mobility of the domain walls [20]. Besides, the Nb^{5+} might be acting as a softer in this system, enhancing d_{33}, kp and ε_r. However, with higher doping contents, the grain size begins decreasing and generates internal stresses, which in turn, inhibit domain wall motion [5]. On the other hand, the strong interaction between grain boundaries and domain walls decreases the domain wall mobility [21]. Ultimately, the two factors lead to reductions in dielectric and piezoelectric properties, such as d_{33}, kp and ε_r. Compare the four sintering temperature, ceramics sintered at 1,150 °C have poor properties, that may be the sintering temperature is too low to have a high density, for the common PZT based ceramics are used sintered at 1,200 °C. The optimal sintering temperature for PZT–SKN and PZT–SNN is 1,175 °C and the relative lower temperature compared with PZT ceramics is resulted from the addition of SKN/SNN. Although the piezoelectric and dielectric properties of PZT–SNN are little lower than PZT–SKN (the optimal values of d_{33}, kp and ε_r for PZT–SKN is 468pC/N, 0.64 and 2,169.05, while the PZT–SNN is 448pC/N, 0.63 and 2,126.32, respectively), both ceramics can be called a favorable material.

Figure 4a, b presents the variation of polarization as function of compositions for samples sintered at 1,175 °C.

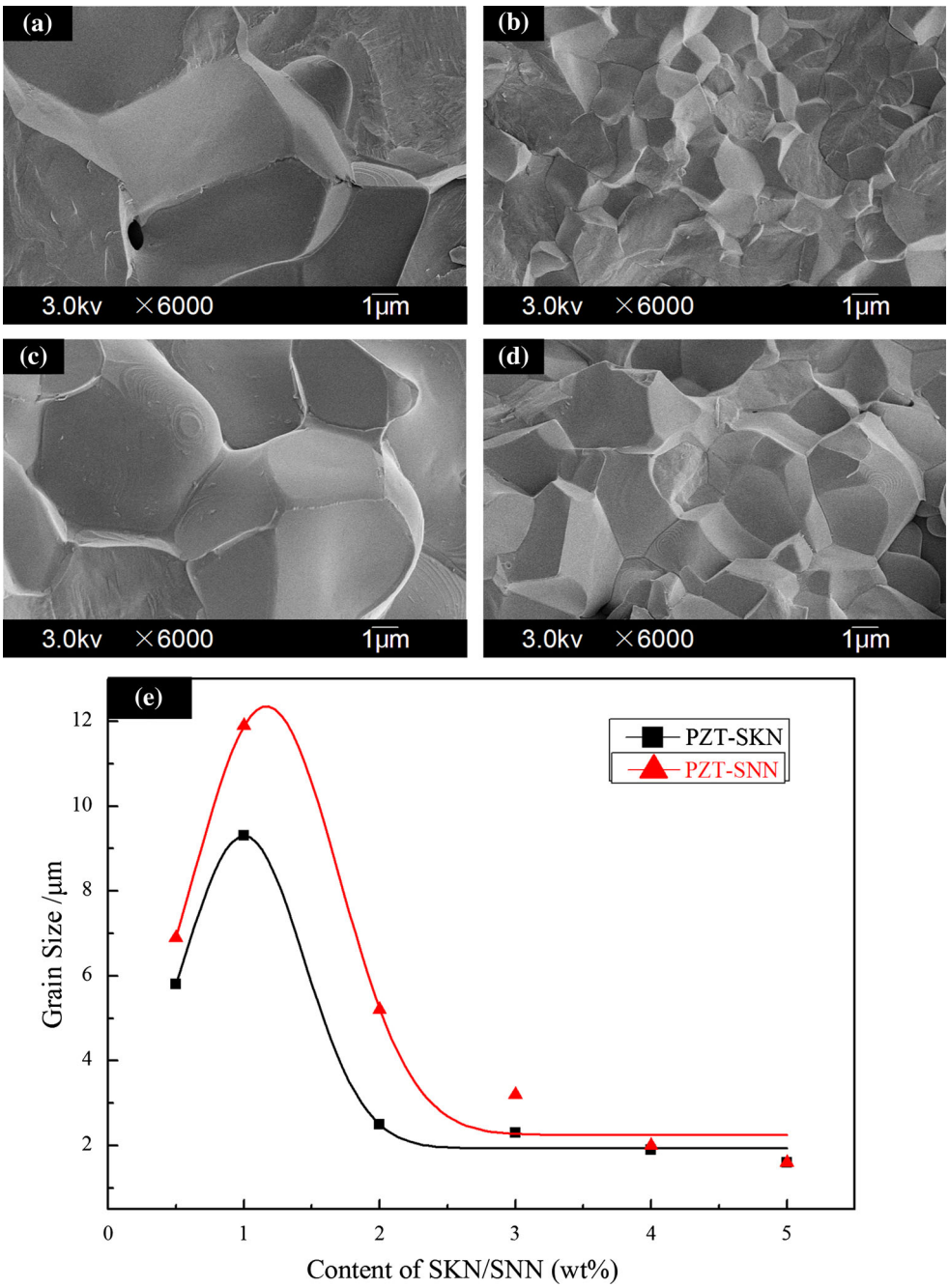

Fig. 2 Fracture surface SEM images of $(1 - x)Pb(Zr_{0.53},Ti_{0.47})O_3$–$xSr(K_{0.25},Nb_{0.75})O_3$ and $(1 - y)Pb(Zr_{0.53},Ti_{0.47})O_3$–$ySr(Na_{0.25},Nb_{0.75})O_3$ with different SKN/SNN contents sintered at 1,175 °C for 2 h: **a** x = 0.01, **b** x = 0.02, **c** y = 0.01, **d** y = 0.02 and **e** plot of grain size

The shape of the hysteresis loops indicates that all samples are of typical ferroelectrics. At an electric field 25 kV/cm, most P–E plots are well-saturated. The round shape hysteresis loop of 0.995PZT–0.005SKN/0.995PZT–0.005SNN sample become square-like with an increase in SKN/SNN doping and the feature of remanent polarization *Pr* for all samples is well fitted with the variation tendency of dielectric and piezoelectric properties showed in Fig. 4. This change in the shape of loop is related to the defect dipoles and grain boundary, which act as pinning sites for domain wall movement and decreased the remanent polarization values. Defect dipoles are formed by acceptor ions and oxygen vacancies. The oxygen vacancies can be caused by K^+ or Na^+ doped, besides, they may also be produced due to loss of oxygen from the crystal lattice during sintering at high temperature [22]. For the ceramic system, the grain size decreased with increasing the SKN/SNN contents, which produce more grain boundaries. The maximum value of *Pr* is 40.65 μC/cm^2 for PZT–SKN ($x = 0.01$) and 39.81 μC/cm^2 for PZT–SNN ($y = 0.002$), respectively, and the relative low *Ec* values of both contents mean that they could be polarized rather easily.

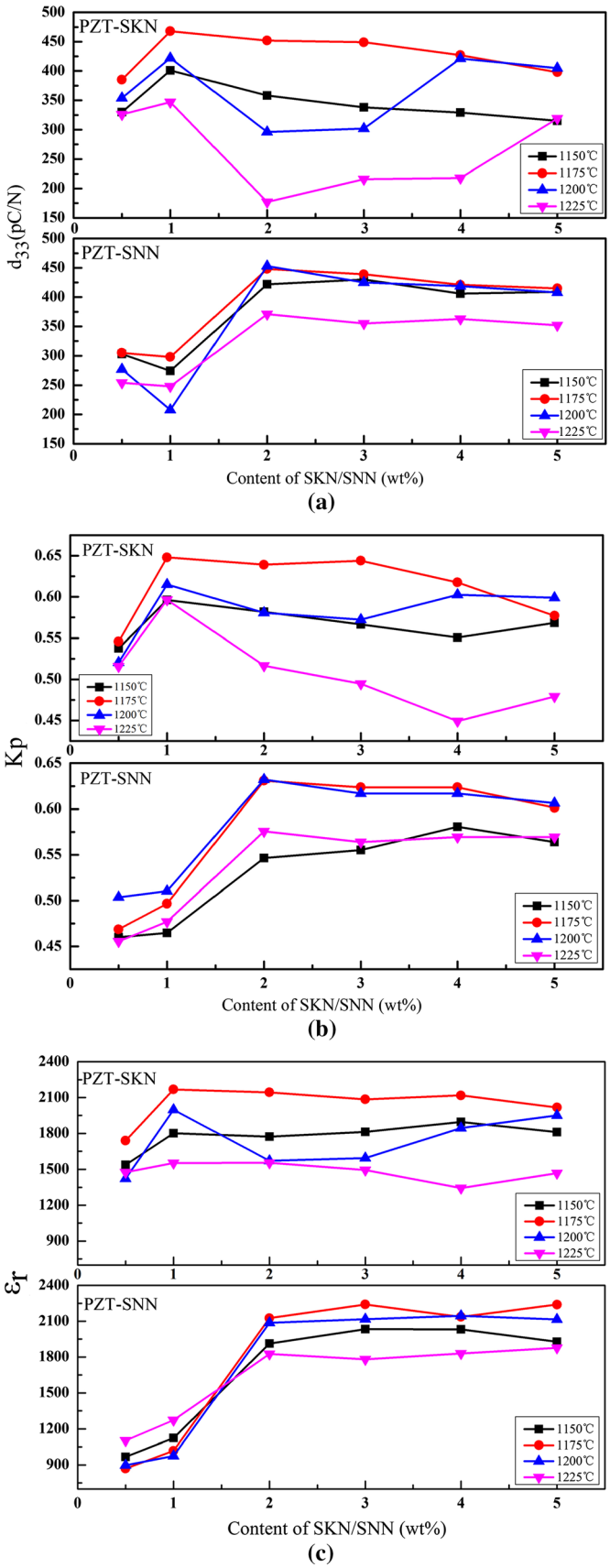

Fig. 3 Piezoelectric and dielectric properties of PZT–SKN/PZT–SNN with various amount of SKN/SNN contents with sintered from 1,175 to 1,225°C for 2 h: **a** piezoelectric constant (d_{33}), **b** electromechanical coupling factor (kp) and **c** dielectric constant (ε_r)

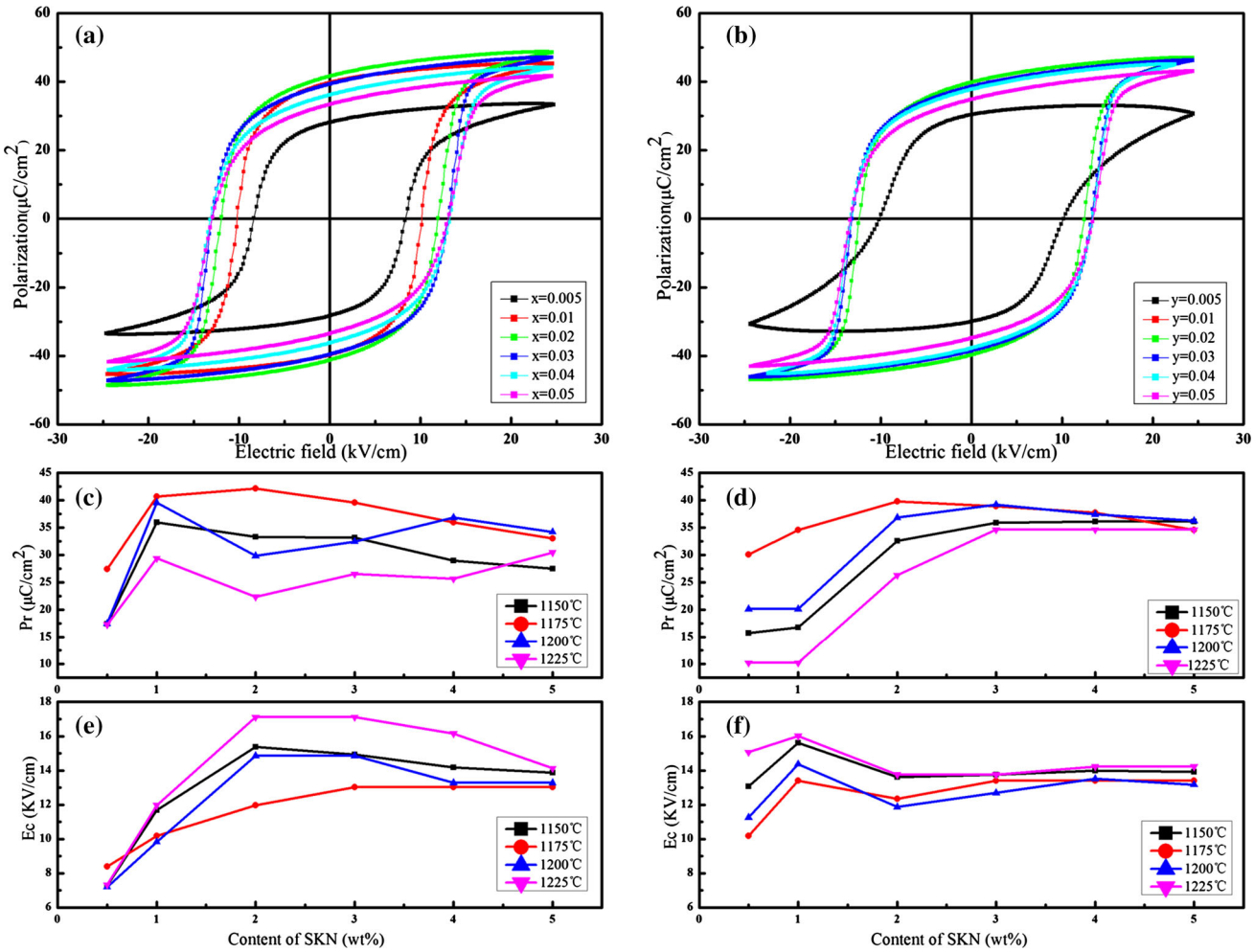

Fig. 4 **a**, **b** Ferroelectric hysteresis loops of $(1-x)$PZT–xSKN and $(1-y)$PZT–ySNN ceramics sintered at 1,175 °C; **c–f** the remanent polarization *Pr* and coercive field *Ec* for both ceramics sintered at different+ temperature

The temperature dependence of the dielectric constant at a measurement frequency of 1 kHz for $(1-x)$PZT–xSKN and $(1-y)$PZT–ySNN ceramics is displayed by the curves in Fig. 5. With increasing SKN/SNN, a reduction of Curie temperature is observed and finally shifts toward room temperature. This can be attributed to Sr and Nb containing in SKN/SNN, which have an obvious effect to decrease the Curie temperature and broaden the peak [22–24]. The inset of Fig. 6 is the profile of tendency of Curie temperature. Through a linear fitting, we can gain that the slop of the PZT–SKN's is about 17.5 °C/mol%, while the PZT–SNN is 20.4 °C/mol%. Particularly, the values of the peak permittivity have a same trend with the variation of grain size and have an abrupt increase at 1 % content. This change may be related to the distribution of ions having different ionic radii in the same sublattice of complex compound with a perovskite structure [25]. This observation is consistent with the reported effects of grain size on PZT ceramics [12]. The Curie temperature is over 290 °C for all contents means that PZT–SKN and PZT–SNN based devices could be used in room temperature or relative higher (about 150 °C).

3.3 Humidity resistance

In order to determine the humidity-resistance characteristics of the ceramics, the samples sintered at 1,175 °C were immerged into distilled water for different durations [26]. The variations of the piezoelectric coefficient d_{33} are listed in Table 1. From the data we can see that all d_{33} show different degrees of decreasing. Figure 6 is the variation curve of the piezoelectric coefficient d_{33} for 0.98PZT–0.02SKN and 0.98PZT–0.02SNN. It can be seen that piezoelectric properties of 0.98PZT–0.02SNN ceramic

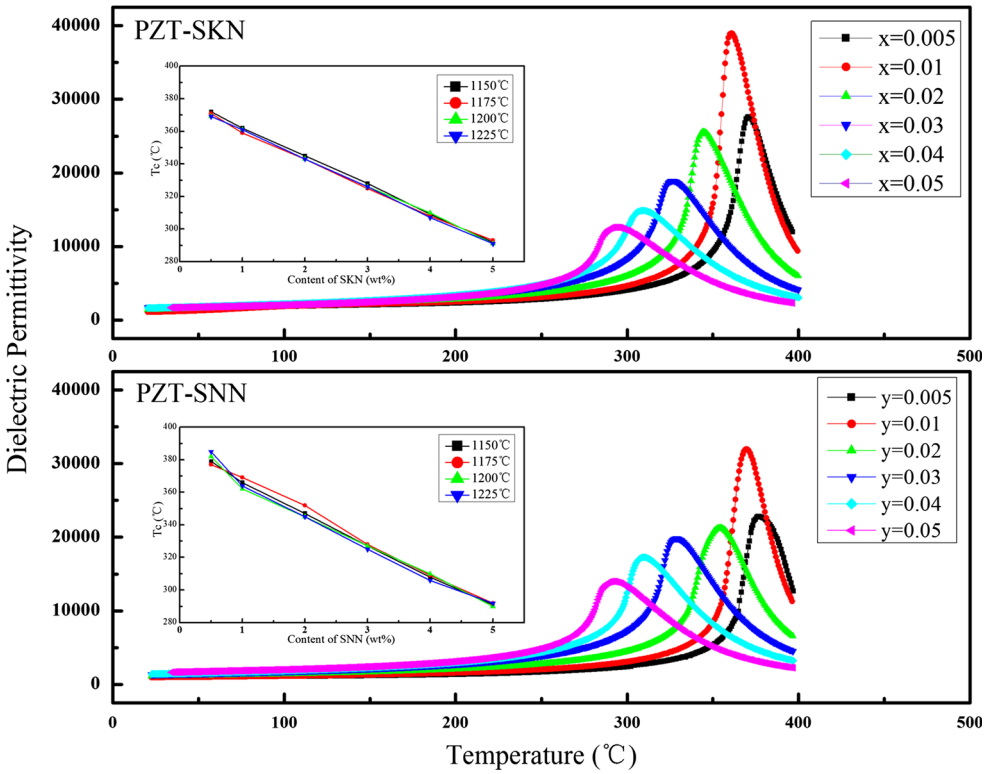

Fig. 5 Temperature dependence of dielectric constant (ε_r) at 1 kHz for $(1-x)$PZT–xSKN/$(1-y)$PZT–ySNN samples sintered at 1,175 °C

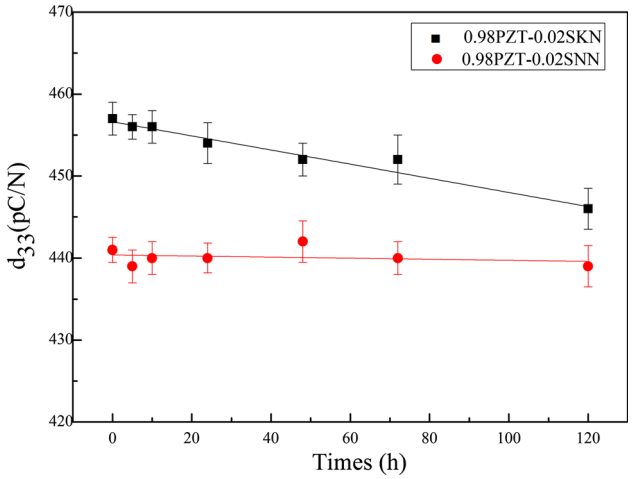

Fig. 6 The variation tendency of the piezoelectric coefficient d_{33} for 0.98PZT–0.02SKN and 0.98PZT–0.02SNN ceramics when immerged into distilled water for different durations

shows no obvious reduction after 120 h of immersion while 0.98PZT–0.02SKN decreases by 2.4 %, nearly six times of 0.98PZT–0.02SNN. For other components ceramics, PZT–SKN also has a large decline than PZT–SNN. That may be results from the hygroscopy which sodion is lower than potassium ion. As a result, PZT–SNN ceramics may have a better practical application than PZT–SKN for its higher humidity-resistance characteristic.

Table 1 Values of d_{33} of the PZT–SKN/PZT–SNN ceramics after different periods of immersion

	Initial	5 h	10 h	24 h	48 h	72 h	120 h
x							
0.005	398	398	397	396	395	393	390
0.01	473	472	474	469	469	467	463
0.02	457	456	456	454	452	452	446
0.03	449	447	446	446	442	440	436
0.04	432	431	432	431	431	421	421
0.05	404	403	403	404	397	396	394
y							
0.005	343	339	338	338	337	334	337
0.01	302	300	301	299	297	297	296
0.02	441	439	440	440	442	440	439
0.03	432	434	436	439	436	432	427
0.04	419	418	419	419	419	417	413
0.05	401	404	406	406	404	399	393

4 Conclusions

$(1-x)$Pb$(Zr_{0.53},Ti_{0.47})O_3$–xSr$(K_{0.25},Nb_{0.75})O_3$ and $(1-y)$Pb$(Zr_{0.53},Ti_{0.47})O_3$–ySr$(Na_{0.25},Nb_{0.75})O_3$ (where $x = y =$ 0.005, 0.01, 0.02, 0.03, 0.04 and 0.05) were produced with pure perovskite structure through conventional solid-state method. Both ceramics show excellent dielectric and

piezoelectric properties and the maximum are obtained at 1,175 °C for 1 % SKN and 2 % SNN. The optimal values of d_{33}, kp, ε_r and Tc for 0.99PZT–0.01SKN is 468pC/N, 0.64, 2,169.05 and 360 °C while the 0.98PZT-0.02SNN is 448pC/N, 0.63, 2,126.32 and 354 °C, respectively. The SKN and SNN both have an effect of decreasing the grain size, lowing the sintering and Curie temperature, besides, SNN has a superior effect than SKN. Importantly, the PZT–SNN has a higher humidity resistance than PZT–SKN, which means it may have a better practical application. The favorable dielectric and piezoelectric properties together with the high Cuie temperature and relative low hygroscopy of 0.98PZT–0.02SNN make itself suitable for fabrication of multilayer piezoelectric devices cofiring with LTCC materials and compatible low-melting-point electrodes (i.e., Ag).

Acknowledgments This work was financially supported by National Natural Science Foundation of China (11372133), NUAA Fundamental Funds (NS2013008), Fundamental Research Funds for the Central Universities (NJ20140012), The State Key Laboratory Program under Grant (MCMS-0514K01), A Project Funded by the Priority Academic Program Development of Jiangsu Higher Education Institutions (PAPD).

References

1. M. Pereira, A.G. Peixoto, M.J.M. Gomes, Effect of Nb doping on the microstructural and electrical properties of the PZT ceramics. J. Eur. Ceram. Soc. **21**, 1353–1356 (2001)
2. D.D. Wan, Q. Li, J.Y. Choi, J.W. Choi, Y. Yang, S.J. Yoon, Low-temperature sintered Pb(Zr, Ti)O_3–Pb(Mn, Sb)O_3–Pb(Zn, Nb)O_3 for multilayer ceramic actuators. Jpn. J. Appl. Phys. **49**, 071503 (2010)
3. L. Qiu, S.F. Yuan, X.L. Shi, T.X. Huang, Design of piezoelectric transducer layer with electromagnetic shielding and high connection reliability. Smart Mater. Struct. **21**, 075032 (2012)
4. C.A. Randall, A. Kelnberger, G.Y. Yang, R.E. Eitel, T.R. Shrout, High strain piezoelectric multilayer actuators—a material science and engineering challenge. J. Electroceram. **14**, 177–191 (2005)
5. N.J. Donnelly, T.R. Shrout, C.A. Randall, Addition of a Sr, K, Nb (SKN) combination to PZT(53/47) for high strain applications. J. Am. Ceram. Soc. **90**, 490–495 (2007)
6. B.S. Li, G.R. Li, S.C. Zhao, L.N. Zhang, A.L. Ding, Characterization of the high-power piezoelectric properties of PMnN–PZT ceramics using constant voltage and pulse drive methods. J. Phys. D Appl. Phys. **38**, 2265–2270 (2005)
7. F. Gao, L.H. Cheng, R.Z. Hong, J.J. Liu, C.J. Wang, C.S. Tian, Crystal Structure and Piezoelectric Properties of xPb($Mn_{1/3}Nb_{2/3}$)O_3–(0.2 − x)Pb($Zn_{1/3}Nb_{2/3}$)O_3–0.8Pb($Zr_{0.52}Ti_{0.48}$)O_3 Ceramics. Ceram. Int. **35**, 1719–1723 (2009)
8. G. Helke, S. Seifert, S.J. Cho, Phenomenological and structural properties of piezoelectric ceramics based on xPb(Zr, Ti)O_3–(1 – x) Sr($K_{0.25}$, $Nb_{0.75}$)O_3 (PZT/SKN) solid solutions. J. Eur. Soc. **19**, 1265–1268 (1999)
9. D. Yuan, Y. Yang, Q. Hu, Y. Wang, Structures and properties of Pb($Zr_{0.5}Ti_{0.5}$)O_3–Pb($Zn_{1/3}Nb_{2/3}$)O_3–Pb($Ni_{1/3}Nb_{2/3}$)O_3 ceramics for energy harvesting devices. J. Am. Soc. **97**(12), 3999–4004 (2014)
10. R.A. Langman, R.B. Runk, S.R. Butler, Isothermal grain growth of pressure-sintered PLZT ceramics. J. Am. Soc. **56**, 486–488 (1973)
11. N. Kim, Grain size effect on the dielectric and piezoelectric properties in compositions which are near the morphotropic phase boundary of lead zirconate-titanate based ceramics, Ph.D. thesis, The Pennsylvania State University, 1994
12. C.A. Randall, N. Kim, J.P. Kucera, W.W. Cao, T.R. Shrout, Intrinsic and extrinsic size effects in fine-grained morphotropic-phase-boundary lead zirconate titanate ceramics. J. Am. Soc. **81**, 677–688 (1998)
13. R.J. Brook, The impurity-drag effect and grain growth kinetics. Scripta Metall. **2**, 375–378 (1968)
14. N.J. Donnelly, T.R. Shrout, C.A. Randall, Properties of (1 − x)PZT–xSKN ceramics sintered at low temperature using Li_2CO_3. J. Am. Soc. **91**, 2182–2188 (2008)
15. R.B. Atkin, R.M. Fulrath, Point defects and sintering of lead zirconate–titanate. J. Am. Soc. **54**, 265–270 (1971)
16. T.C. Che, C.S. Yuan, L.C. Hsien, Doping effects of Nb additives on the piezoelectric and dielectric properties of PZT ceramics and its application on saw device. Sens. Actuators A **113**, 198–203 (2004)
17. M.N. Rahaman, *Ceramic processing and sintering* (CRC Press, Boca Raton, 2003)
18. G. Srivastava, A. Goswami, A.M. Umarji, Temperature dependent structural and dielectric investigations of $PbZr_{0.5}Ti_{0.5}O_3$ solid solution at the morphotropic phase boundary. Ceram. Int. **39**, 1977–1983 (2013)
19. K. Volkan, C. Ibrahim, T. Muharrem, Dielectric and piezoelectric properties of PZT ceramics doped with strontium and lanthanum. Ceram. Int. **37**, 1265–1275 (2011)
20. M.M.S. Pojucan, M.C.C. Santos, F.R. Pereira, M.A.S. Pinheiro, M.C. Andrade, Piezoelectric properties of pure and (Nb^{5+} + Fe^{3+}) doped PZT ceramics. Ceram. Int. **36**, 1851–1855 (2010)
21. W.L. Zhang, R.E. Eitel, Low-temperature sintering and properties of 0.98PZT–0.02SKN ceramics with $LiBiO_2$ and CuO addition. J. Am. Soc. **94**, 3386–3390 (2011)
22. Volkan Kalem, Muharrem Timucin, Structural, piezoelectric and dielectric properties of PSLZT–PMnN ceramics. J. Eur. Ceram. Soc. **33**, 105–111 (2013)
23. B. Jaffe, W.R. Cook, H. Jaffe, *Piezoelectric ceramics* (Amademic Press, NewYork, 1971)
24. H. Zheng, I.M. Reaney, W.E. Lee, Effects of strontium substitution in Nb-doped PZT ceramics. J. Eur. Ceram. Soc. **21**, 1371–1375 (2001)
25. Vladimir Koval, Carlos Alemany, Jaroslav Briancin, Helena Brunckova, Dielectric properties and phase transition behavior of xPMN–(1 − x)PZT ceramic systems. J. Electroceram. **10**, 19–29 (2003)
26. L.M. Zheng, J.F. Wang, C.M. Wang, Thermal stability and humidity resistance of $ScTaO_4$ Modified ($K_{0.5}Na_{0.5}$)NbO_3 ceramics. Chin. Phys. Lett. **26**, 127701 (2009)